Shipley, G. G. (1973) in *Biological Membranes* (Chapman, D., & Wallach, D. F. H., Eds.) Vol. 2, pp 1–89, Academic, London and New York.
Tanford, C. (1973) *The Hydrophobic Effect*, Wiley-Interscience, New York.
Weast, R. C. (1980) *Handbook of Chemistry and Physics*, 61st ed., CRC Press, Boca Raton, FL.
Yue, B. Y., Jackson, C. M., Taylor, J. A. G., Mingins, J., & Pethica, B. A. (1976) *J. Chem. Soc., Faraday Trans. 1*, 2685–2693.

Calcium Binding to Mixed Phosphatidylglycerol–Phosphatidylcholine Bilayers As Studied by Deuterium Nuclear Magnetic Resonance†

Peter M. Macdonald and Joachim Seelig*
Department of Biophysical Chemistry, Biocenter of the University of Basel, CH-4056 Basel, Switzerland
Received May 14, 1986; Revised Manuscript Received November 13, 1986

ABSTRACT: The binding of calcium to bilayer membranes composed of mixtures, in various proportions, of 1-palmitoyl-2-oleoyl-*sn*-glycero-3-phosphocholine (POPC) plus 1-palmitoyl-2-oleoyl-*sn*-glycero-3-phosphoglycerol (POPG) was investigated by using atomic absorption spectroscopy and deuterium nuclear magnetic resonance. The number of bound calcium ions, X_2, was determined in the low calcium concentration range (up to 100 mM) via atomic absorption spectroscopy. Simultaneous measurements of the deuterium magnetic resonance spectra of POPC, specifically deuteriated at the α-methylene segment of the choline head group, revealed a linear relationship between the quadrupole splitting, $\Delta\nu_Q$, and X_2 for each particular proportion of POPC–POPG. The amount of bound calcium was then determined at much greater calcium concentrations, where the atomic absorption spectroscopy measurements were unreliable, using deuterium magnetic resonance. At low Ca^{2+} concentrations, the amount of bound Ca^{2+} increased linearly with increasing proportion of POPG, demonstrating an electrostatic contribution to Ca^{2+} binding. At high Ca^{2+} concentrations, the calcium binding isotherms exhibited saturation behavior with a maximum binding capacity of 0.5 Ca^{2+} and 1.0 Ca^{2+} per phospholipid for pure POPC and mixtures of POPC–POPG, respectively. Simultaneous deuteriation of POPG and POPC showed that both lipids remained in a fluidlike lipid bilayer at all Ca^{2+} concentrations tested. Any phase separation of quasi-crystalline Ca^{2+}–POPG clusters could be excluded. The residence time of Ca^{2+} at an individual head group binding site was shorter than 10^{-6}–10^{-5} s. Thus, Ca^{2+} ions accumulate near the negatively charged POPG–POPC membrane surface but move freely in a "trough" of the electrical potential. The effective surface charge density, σ, could be determined from the measured amount of bound Ca^{2+}. Subsequently, the surface potential, ψ_0, and the concentration of free Ca^{2+} ions at the plane of ion binding could be calculated by employing the Gouy–Chapman theory. The availability of these parameters allowed a rigorous evaluation of various models for the chemical contribution to Ca^{2+} binding. For mixed POPC–POPG bilayers, a simple Langmuir adsorption model yielded the best fit to the experimental data, and the binding constants were 19.5 and 18.8 M^{-1} for POPG contents of 20 and 50 mol %, respectively. Sodium binding was comparatively weak with a binding constant of 0.6–0.85 M^{-1}. The values of the calcium association constants indicate that the increased binding of calcium with increasing proportion of POPG is predominantly an electrostatic effect, rather than the result of an intrinsically greater affinity of POPG for calcium. Calcium was able to reduce the surface potential by binding and neutralizing negative surface charges in addition to having a screening effect.

Negatively charged lipids are common components of biological membranes and can be expected to attract and to bind calcium and other ions (Eisenberg et al., 1979; Lau et al., 1981). The binding of cations may alter the conformation and physical properties of membrane lipids [e.g., see Fleming & Keough (1983)], as well as the electrical and functional properties of the membrane proper (McLaughlin, 1977), and can have important physiological consequences (McLaughlin, 1977; Scarpa & Carafoli, 1979).

Previously, the various techniques employed to study the binding of ions to membrane surfaces have not measured directly the amount of bound ion but rather have inferred this quantity indirectly from measurements of such parameters as the electrophoretic mobility (Eisenberg et al., 1979; Lau et al., 1981; McLaughlin et al., 1983), the electrostatic interbilayer repulsive force (Lis et al., 1981a,b; Oshima et al., 1982), or the competition with lanthanide shift reagents (Grasdalen et al., 1977). A direct measurement of the amount of bound ion can be obtained, however, over a limited concentration range, by using atomic absorption spectroscopy. The available range of concentrations can then be greatly extended by using deuterium nuclear magnetic resonance (^2H NMR).[1] The change in the quadrupolar splitting in spectra of specifically deuteriated lipid polar head groups, which occurs

†Supported by Swiss National Science Foundation Grant 3.014.84. P.M.M. was the recipient of a Medical Research Council of Canada postdoctoral fellowship.

[1] Abbreviations: NMR, nuclear magnetic resonance; POPC, 1-palmitoyl-2-oleoyl-*sn*-glycero-3-phosphocholine; POPG, 1-palmitoyl-2-oleoyl-*sn*-glycero-3-phosphoglycerol; POPA, 1-palmitoyl-2-oleoyl-*sn*-glycero-3-phosphatidic acid; Tris-HCl, tris(hydroxymethyl)aminomethane hydrochloride.

0006-2960/87/0426-1231$01.50/0

upon ion binding, is first calibrated with respect to the amount of bound ion, obtained via atomic absorption spectroscopy. This relationship is then extrapolated in order to interpret ^2H NMR spectra measured over a much larger concentration range (Altenbach & Seelig, 1984, 1985).

The association of ions with membrane lipids involves both a chemical equilibrium, as represented in a particular model of ion binding, and electrostatic considerations, as exemplified by the Gouy–Chapman theory (Aveyard & Haydon, 1973; McLaughlin, 1977). Recently, using this approach, it has been possible to describe quantitatively the adsorption of calcium ions to neutral phosphatidylcholine membranes and to successfully differentiate various models of ion binding (Altenbach & Seelig, 1984).

In this report, we extend these investigations of calcium–lipid interactions to the biologically important case of mixtures of negatively charged and zwitterionic lipids, i.e., phosphatidylglycerol and phosphatidylcholine. Phosphatidylglycerol, which is the predominant negative lipid of bacterial (Lennarz, 1970) and plant (Hitchcock & Nichols, 1971) membranes, possesses a polar head group that is structurally simpler than its negatively charged mammalian counterpart phosphatidylserine (Rouser et al., 1968) and displays less complex phase behavior in mixtures with phosphatidylcholine than does phosphatidylserine (McElhaney, 1982; Borle & Seelig, 1985). Furthermore, the molecular species of phospholipids chosen, 1-palmitoyl-2-oleoyl-*sn*-glycero-3-phosphocholine (POPC) and 1-palmitoyl-2-oleoyl-*sn*-glycero-3-phosphoglycerol (POPG), closely resemble naturally occurring lipid species both in terms of the constituent fatty acyl groups and their positional distribution (Strickland, 1973) and also in their thermotropic phase behavior (Silvius, 1982).

The results reported here describe the determination of the binding of calcium to mixtures, in various proportions, of POPG with POPC using the combined atomic absorption spectroscopy and ^2H NMR techniques developed previously (Altenbach & Seelig, 1984). The resulting calcium binding isotherms are analyzed in terms of both chemical binding and electrostatic attraction, with a comparison of various chemical models of calcium binding.

Theory

Consider first fully hydrated, liquid-crystalline lipid bilayers composed of the zwitterionic phospholipid POPC. Since POPC carries no net charge, the membrane surface is electrically neutral. If we now add to the buffer an ion, such as calcium, which has a chemical affinity for POPC, some fraction of the POPC molecules will associate with calcium ions. The membrane surface will now carry a net positive charge of surface charge density σ and an associated positive membrane surface potential ψ_0. The charged membrane surface repels ions of like charge and attracts ions of opposite charge. Therefore, the interfacial concentration of calcium ions in the vicinity of the positively charged membrane surface will be less than the bulk concentration in the bathing solution.

Returning to the original POPC bilayers with no bound ions, consider next the effect of adding to these bilayers a negatively charged lipid such as POPG. The membrane surface will now carry a net negative charge. If the proportion of POPG is progressively increased, the surface charge density and the membrane surface potential increase negatively until maximum negative values are reached for pure POPG bilayers. Now, consider again the addition of calcium ions. Due to the negative surface charge density, Ca^{2+} ions will be attracted to the membrane surface, and the Ca^{2+} concentration at the membrane–water interface will exceed the equilibrium concentration in the bulk solution. In addition, some calcium will be bound chemically to the lipid head groups. Thus, the initial negative surface charge of the lipid membranes is reduced by electrostatic screening and by chemical binding. This view of ion binding emphasizes the necessity of considering both the chemical equilibrium and the electrostatic aspects of ion binding.

At the conjunction of these two considerations is the surface charge density (σ) which both is effected by and is an effector of ion binding. The effective surface charge density is a function of both the amount of negative lipid and bound positive ions, such that

$$\sigma = (e_0/S)(-X_{PG} + \sum_i z_i X_i) \quad (1)$$

where e_0 is the electronic charge, S the surface area per lipid molecule (assumed to be equal for POPC and POPG), X_{PG} the mole fraction of negatively charged phosphatidylglycerol, and X_i the mole fraction of bound ion i with valence z_i (X_i = moles of bound ion i per mole of total lipid). It is assumed that the negatively charged lipid is completely dissociated. The summation is over all bound ions i, so that the binding of ions other than calcium (e.g., sodium) may also be considered. Assuming identical surface areas of $S = 68$ Å^2 for both POPG and POPC (Altenbach & Seelig, 1984; Borle & Seelig, 1985), eq 1 takes the form

$$\sigma = 0.236(-X_{PG} + \sum_i z_i X_i)\ \text{C m}^{-2} \quad (2)$$

The surface charge density, σ, creates a surface potential, ψ_0, which can be calculated with the Gouy–Chapman theory (Aveyard & Haydon, 1973; McLaughlin, 1977):

$$\sigma^2 = 2000\epsilon_0\epsilon_R RT\sum_i C_{i,eq}(e^{-z_i F_0\psi_0/RT} - 1) \quad (3)$$

where ϵ_R is the dielectric constant of water, ϵ_0 the permittivity of free space, R the gas constant, T the absolute temperature, $C_{i,eq}$ the equilibrium concentration of ion i in the bulk aqueous phase, and F_0 the Faraday constant. The summation is over all ions i in solution, i.e., including anions.

Having calculated the surface potential, the concentration, $C_{i,M}$, of a particular ion at the plane of ion binding, i.e., in the solution adjacent to the membrane surface, can be obtained from the Boltzmann equation:

$$C_{i,M} = C_{i,eq}\exp(-z_i F_0\psi_0/RT) \quad (4)$$

We are now in a position to analyze the chemical aspects of ion binding. We limit the discussion to the competitive binding of Ca^{2+} and Na^+ and denote with X_1 (X_2) the mole fraction of bound Na^+ (Ca^{2+}) measured as moles of bound ion per mole of total lipid. If X_L is the mole fraction of free lipid, mass conservation of the lipid requires

$$X_L + X_1 + nX_2 = 1 \quad (5)$$

Equation 5 is based on the assumption that the Ca^{2+} binding sites are composed of n lipids each, while the Na^+ binding site is identical with a single lipid. The law of mass action for the binding to a membrane surface takes the form [cf. Stankowski (1983a,b, 1984)]:

$$K_i C_{i,M} = X_i/X_F \quad (6)$$

where K_i is the binding constant (Ca^{2+}, K_2; Na^+, K_1) and $C_{i,M}$ and X_i have been defined above. The new parameter in eq 6 is X_F, the mole fraction of free binding sites. Only if the metal ion complexes with a single lipid is the mole fraction of free binding sites, X_F, identical with the mole fraction of free lipids, X_L. A more complex situation arises if the metal ion requires a binding site of n lipids. Under these conditions,

rather elaborate statistical calculations may be needed to relate the concentration of free lipid to the concentration of free binding sites. Here we consider two approximate models which we call nonspecific binding and specific binding, respectively.

Nonspecific Binding. A metal ion binds to a binding site composed of n lipids. The mole fraction of binding sites, X_F, is obtained from the mole fraction, X_L, of free lipid according to

$$X_F = X_L/n \quad (7)$$

It has been pointed out that eq 7 (which forms the basis for the so-called Scatchard plots) is strictly valid only for identical, independent, and nonoverlapping binding sites [cf. Stankowski (1983)]. If a metal ion binds to n identical lipids, then the free lipids usually do not occur in clusters of n. Hence, the concentration of free binding sites, X_F, is expected to be larger than predicted by eq 7. However, the present investigation is concerned with mixtures of lipids. For the sake of argument, we consider a situation in which a metal ion binds to a "lipid pair" composed of a negatively charged lipid and a neutral lipid. Hence, an individual binding site is composed of two lipids. For an equimolar mixture, the number of free binding sites X_F (lipid pairs) would thus be $X_F = X_L/2$ where X_L is the total free lipid concentration (sum of both lipids). Since the binding mechanism is completely unknown, it is necessary to test eq 7 for various n even though $n = 1$ would be the preferred choice for theoretical reasons.[2]

Specific Binding. By analogy with chemical reactions in solution, one may postulate that

$$X_F = X_L^m \quad (8)$$

where m is an integer and denotes the number of lipid ligands for a given metal ion. Equations 7 and 8 may be combined in the general form

$$X_F = (X_L/n)^m \quad (9)$$

For the case of sodium, we assume nonspecific binding with $n = 1$, and the law of mass action takes the form

$$K_1 C_{1,M} = X_1/X_L \quad (10)$$

For Ca^{2+} binding, we shall use the approximation (eq 9), yielding

$$K_2 C_{2,M} = X_2/(X_L/n)^m \quad (11)$$

Combination of eq 5, 10, and 11 eliminates X_1 and X_L and leads to

$$X_2/(1 - nX_2)^m = C_{2,M}(K_2/n^m)/(1 + K_1 C_{1,M})^m \quad (12)$$

As will be discussed later, X_2 can be measured with atomic absorption spectroscopy and ^2H NMR. In this general form, the specific and nonspecific binding models are differentiated by the following conditions. For nonspecific binding, m always equals unity regardless of the value of n. For specific binding, m always equals n. Note that this condition makes the specific binding model equivalent to the Bragg–Williams approximation which, as discussed by Stankowski (1983a), is highly appropriate to describe the surface binding of small ligands (low values of n) to a lattice of high coordination number (i.e., the hexagonal lattice of a lipid bilayer surface). Finally, for the case of $n = 1$, both models reduce to a simple Langmuir adsorption isotherm.

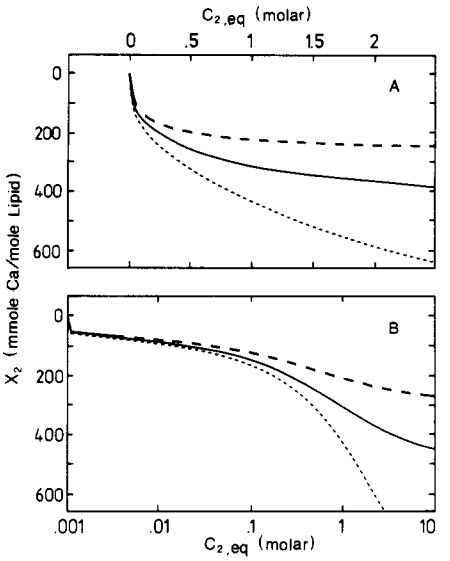

FIGURE 1: Computer simulations of the calcium binding isotherm expected for lipid/ion stoichiometries of 1, 2, or 3. Other simulation expected for specific lipid/ion stoichiometries of 1, 2, or 3 (dashed, solid, or dotted curve, respectively). Other parameters were K_2 = 20.0 M^{-1}, K_1 = 0 M^{-1}, mole fraction of negative lipid = 0.20, and T = 298 K.

In later sections, we shall compare the experimentally determined binding isotherm X_2 vs. $C_{2,eq}$ with computer simulations based on eq 12. The sensitivity of this comparison is illustrated in Figure 1 which displays theoretical binding isotherms calculated with eq 12 under the condition of $n = m$ with n = 1, 2, or 3. The effective binding constant $K^* = k_2/n^m$ was assumed to be equal for all three curves, and sodium binding was neglected. The interfacial Ca^{2+} concentration, $C_{2,M}$, was calculated with the Gouy–Chapman theory and the Boltzmann equation as above.

The great differences in the calcium binding isotherms are clearly evident. Furthermore, the necessity of investigating as great a range of calcium concentrations as possible becomes apparent in this figure, since the extreme differences in the expected ion binding behavior for different values of n, so evident at high calcium concentrations, virtually vanish below 100 mM calcium (cf. Figure 1B).

Materials and Methods

Materials. The following nomenclature is employed for the phosphocholine and phosphoglycerol head group segments:

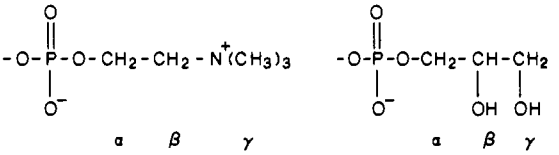

Nondeuteriated 1-palmitoyl-2-oleoyl-*sn*-glycero-3-phosphocholine (POPC), 1-palmitoyl-2-oleoyl-*sn*-glycero-3-phosphoglycerol (POPG), and 1-palmitoyl-2-oleoyl-*sn*-glycero-3-phosphatidic acid (POPA) were purchased from Avanti Polar Lipids, Inc. (Birmingham, AL). POPC was selectively deuteriated at the α-segment and POPG at the β-segment starting from POPA as described by Tamm and Seelig (1983) and Wohlgemuth et al. (1980), respectively. All lipids were subjected to ion-exchange chromatography on CM-52 using the

[2] The binding of tetraphenylphosphonium to bilayers composed of 1-palmitoyl-2-oleoyl-*sn*-glycero-3-phosphocholine can be fit best with eq 7 and n = 8.3 in the range of $0.01 < X_2 < 0.1$ (Altenbach & Seelig, 1985). Similar results have been obtained for tetraphenylborate and two local anesthetics. Although one might object to the use of eq 7 on theoretical grounds, it is an experimental fact that this approximation provides the best empirical fit to a number of binding isotherms. Moreover, the conclusions derived from this analysis could be compared with other methods. In the case of tetraphenylphosphonium, the results were in remarkable agreement with conductivity measurements on black films and with measurements using ion-selective electrodes.

procedure described by Comfurius and Zwaal (1977) prior to their use in an ion binding assay.

Measurement of Calcium Binding by Atomic Absorption Spectroscopy. The calcium binding assay followed the procedure described by Altenbach and Seelig (1984). Typically, a volume of dichloromethane containing 26 μmol of POPC plus POPG in the desired proportion was dried under a stream of nitrogen, and the residual solvent was removed overnight under high vacuum. The lipids were then dispersed in 400 μL of aqueous solution containing 100 mM NaCl and 10 mM Tris-HCl, pH 7.4, plus the desired concentration of $CaCl_2$ by repeated warming to 45 °C and vortexing until a homogeneous suspension was obtained. Equilibrium was achieved by subjecting the samples to repeated cycles of freeze–thaw, maintenance for 48 h at 4 °C, and finally intermittent vortexing over a 6-h period at 25 °C. The suspension was centrifuged for 20 min at 20000*g* in a Sorvall RC-2B centrifuge and the clear supernatant removed with a pipet. The calcium concentration in the supernatant was determined by using a Perkin-Elmer 5000 atomic absorption spectrophotometer. The quantity denoted as X_2, corresponding to the moles of bound calcium per mole of phospholipid, equalled the difference in the amount of calcium present before and after the addition of lipids divided by the molar quantity of lipids. This assay could not be used at calcium concentrations greater than 100 mM since above this concentration the change in calcium content due to binding to lipids was too small to permit accurate determinations. The value of $C_{2,eq}$, which is the thermodynamic equilibrium concentration of free calcium in the bulk solution, corresponded to the calcium concentration of the supernatant after lipid binding.

Deuterium NMR. All ^2H NMR spectra were recorded on a Bruker CXP-300 spectrometer operating at 46.1 MHz, employing a quadrupole echo technique (Davis et al., 1976) and using the experimental conditions described previously (Seelig et al., 1981; Tamm & Seelig, 1983). The lipid pellets resulting from the calcium binding–atomic absorption procedure were transferred in NMR sample tubes and measured without further modification.

Computer Simulations. Experimental calcium binding isotherms (corresponding to $\Delta\nu_Q$ vs. $C_{2,eq}$) were simulated by using a nonlinear least-squares fit program involving a Marquardt routine as described by Bevington (1969). The quality of the fit of simulated binding isotherms to experimental isotherms was expressed as a χ value (in hertz) representing the mean deviation of experimental points from the simulated binding curve.

RESULTS

Employing the atomic absorption spectroscopy–calcium binding assay described under Materials and Methods, the quantity X_2 (equivalent to the moles of calcium bound per mole of lipid) was determined as a function of the equilibrium bulk calcium concentration, $C_{2,eq}$, for mixture of POPC with POPG. The results are plotted in Figure 2. It is immediately apparent that the amount of bound calcium increases distinctly as the proportion of POPG increases. There appear to be two components of calcium binding in the presence of POPG: an initial strong stage of binding at low calcium concentrations followed by further weak binding at progressively higher calcium concentrations. The binding isotherms for POPG-containing membranes appear to reach saturation at Ca^{2+} concentrations between 50 and 100 mM. The useful range of the atomic absorption–calcium binding assay is limited by both the reproducibility and the accuracy of an individual atomic absorption measurement. The difference between two such

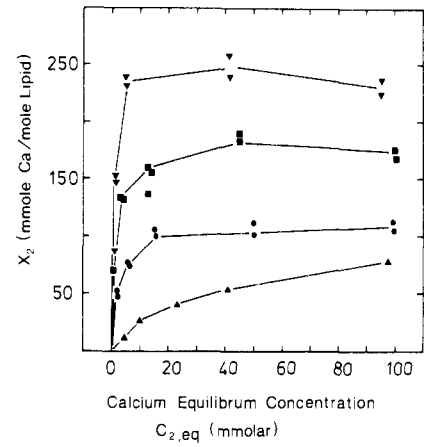

FIGURE 2: Level of calcium binding, X_2 (millimoles of Ca^{2+} per mole of lipid), determined by using atomic absorption spectroscopy, for mixed bilayers containing various proportions of POPC plus POPG as a function of the equilibrium bulk calcium concentration, $C_{2,eq}$. Triangles, 100% POPC; circles, 80% POPC plus 20% POPG; squares, 50% POPC plus 50% POPG; inverted triangles, 20% POPC plus 80% POPG. Proportions are mole percents. The data for 100% POPC were taken from Altenbach and Seelig (1984) (0.1 M NaCl and 0.01 M Tris-HCl, pH 7.4, 25 °C).

determinations, before and after lipid binding, gives a calcium binding datum X_2. The reproducibility of individual determinations was a constant ±5% of the actual solution calcium content. At calcium concentrations higher than 100 mM, this variability becomes large relative to the difference in calcium content due to lipid binding, and the imprecision quickly becomes limiting.

The plateau regions observed in Figure 2 occur well within the range of calcium concentrations at which measuring precision is high. The plateau effect can be measured reproducibly, albeit with larger scatter than at lower calcium concentrations. However, there are a number of lines of evidence which indicate that binding is not truly saturated at these calcium concentrations. We know from ion binding studies using other techniques [i.e., electrophoretic measurements on lipid vesicles (Lau et al., 1981)] that Ca^{2+} binding continues to increase beyond 100 mM. This point is supported by the ^2H NMR measurements to be described below. Moreover, at somewhat higher calcium concentrations, the atomic absorption binding assay indicates that calcium binding actually decreases!

The question which remains then is the following: Why does the atomic absorption binding assay fail to indicate higher binding levels at higher ion concentrations? Control measurements with Ca^{2+} stock solutions showed us that atomic absorption spectroscopy systematically underestimated the calcium content for stock concentrations greater than 20 mM. Moreover, the magnitude of the discrepancy became greater (in percent terms) as the calcium concentration increased. For example, this factor was 5% at 50 mM, was 20% at 100 mM, and rose to as high as 40% at 1 M calcium. Such an effect could be the result of the serial dilutions required to bring the calcium levels down into the concentration range to which the atomic absorption instrument is sensitive. This systematic nonlinear discrepancy effects the measurement of calcium binding as follows. Since we measure the difference in supernatant calcium levels before and after binding to lipids, the percentage by which atomic absorption spectroscopy underestimates the calcium levels before and after lipid binding is also different. In fact, the nonlinear nature of the "undershoot" tends to decrease the difference "before minus after" and thereby leads to serious underestimates of X_2. Furthermore,

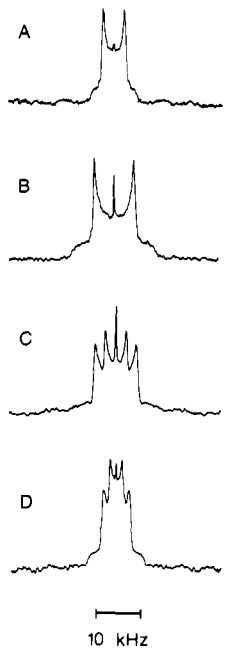

FIGURE 3: ^2H NMR spectra of mixed bilayers containing 50 mol % POPG plus 50 mol % POPC. (A) β-CD-POPG plus POPC (100 mM NaCl and 10 mM Tris-HCl, pH 7.4). (B) POPG plus α-CD_2-POPC (100 mM NaCl and 10 mM Tris-HCl, pH 7.4). (C) β-CD-POPG plus α-CD_2-POPC (100 mM NaCl and 10 mM Tris-HCl, pH 7.4). (D) β-CD-POPG plus α-CD_2-POPC (100 mM $CaCl_2$, 100 mM NaCl, and 10 mM Tris-HCl, pH 7.4).

the larger the actual difference "before minus after" is, the greater the underestimate of X_2. Hence, the shapes of the binding isotherms are altered such that, at higher levels of calcium binding, the apparent binding levels off or even decreases. The range of binding levels which can be measured accurately by using this assay is, therefore, also limited. We consider values of X_2 greater than 100–150 mmol of Ca^{2+}/mol of lipid as approaching this limit. Note that this level of binding is reached at different bulk calcium concentrations for different POPG contents. In using these binding data to calibrate the ^2H NMR measurements of calcium binding, we have relied only on the initial binding data where accuracy and precision are highest.

In Figure 2, the amount of bound Ca^{2+} increases linearly with the membrane POPG content up to calcium concentrations of 50 mM. This result is a first suggestion that for Ca^{2+} concentrations below 50 mM the calcium binding is mainly electrostatic and linearly proportional to the negative surface charge of the membrane.

The limited range of calcium concentrations over which the atomic absorption–calcium binding assay can be applied is insufficient to permit a complete description of calcium binding. Consequently, we have employed ^2H NMR measurements of the head group deuteriated lipids in order to extend the range of calcium concentrations amenable to investigation.

Figure 3 shows a series of ^2H NMR spectra of mixtures of 50 mol % POPG plus 50 mol % POPC in which the positions of the deuterons on the polar head groups have been varied. All spectra display the line shape characteristic of a random dispersion of liquid-crystalline bilayers (Seelig, 1977). In the uppermost spectrum, the deuterons were located at the β-segment of the phosphoglycerol head group of POPG, resulting in a value for the residual quadrupole splitting, $\Delta\nu_Q$, of 4.2 kHz. Immediately below is the spectrum obtained when the deuterons were located at the α-segment of the phosphocholine head group of POPC for which the measured value of $\Delta\nu_Q$ was

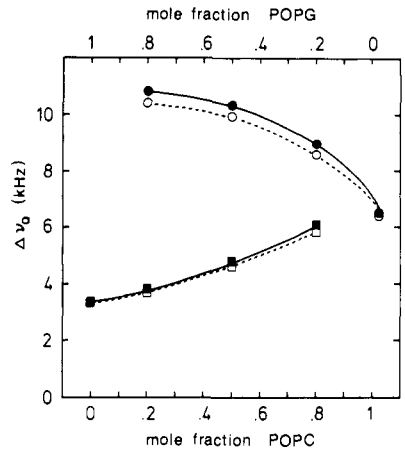

FIGURE 4: Deuterium quadrupole splittings, $\Delta\nu_Q$, of β-CD-POPG and α-CD_2-POPC in mixtures of the two as a function of molar fraction POPC. Solid line: 10 mM Tris-HCl, pH 7.4. Dashed line: 100 mM NaCl and 10 mM Tris-HCl, pH 7.4.

10.0 kHz. The next spectrum, obtained with an equimolar mixture of α-CD_2-POPC and β-CD-POPG, shows two quadrupole splittings corresponding to those observed for the cases in which one or the other of these positions was labeled separately. Clearly, using ^2H NMR, it is possible to monitor the polar head groups of both POPC and POPG independently and simultaneously in mixtures of the two (Borle & Seelig, 1985). In the bottom spectrum, 100 mM $CaCl_2$ was added to an equimolar mixture of α-CD_2-POPC and β-CD-POPG. Again, two quadrupolar splittings are evident, but both have decreased substantially in value relative to their size in the absence of calcium. Significantly, the POPG deuterons remain NMR visible in the presence of 100 mM calcium which demonstrates that the POPG molecules are part of a fluidlike bilayer. The formation of quasi-crystalline Ca^{2+}–POPG clusters can be excluded since this would lead to an almost complete loss of ^2H NMR signal intensity under the measuring conditions employed.

The quadrupole splittings observed with mixtures of head group deuteriated POPC and POPG even in the absence of metal ions are not equal to those observed for pure bilayers of either lipid. This point is evident in Figure 4 where the quadrupole splittings measured in mixtures of α-CD_2-POPC and β-CD-POPG are plotted as a function of the mole fractions of the two lipids. The quadrupole splitting from α-CD_2-POPC increased in a nonlinear fashion from approximately 6.0 kHz at 0 mol % POPG up to approximately 10.5 kHz at 80 mol % POPG. The quadrupole splitting from β-CD-POPG increased from approximately 4.0 kHz at 0 mol % POPC to approximately 6.0 kHz at 80 mol % POPC. The presence of 100 mM NaCl only marginally decreased the quadrupole splittings without regard to the mole fraction of POPC. Similar results have been obtained by Sixl and Watts (1983), who reported, in addition, increased quadrupole splitting for the α-segment of dimyristoylphosphatidylcholine upon mixing with phosphatidylserine. Furthermore, we have observed substantial increases in the quadrupole splittings of the α-segment of head group deuteriated POPC upon mixing with either phosphatidylserine or phosphatidic acid (P. Scherer, A. Seelig, and J. Seelig, unpublished results). This phenomenon would appear to be a general consequence of mixing phosphatidylcholines with negatively charged lipids. The precise origin of this effect, whether due to a perturbation of the water structure at the membrane surface or to an effect of the negative surface potential upon the conformation of the choline head group, remains uncertain. It is clear, however,

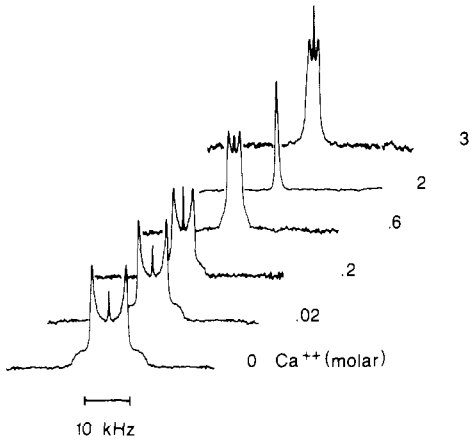

FIGURE 5: ^2H NMR spectra of mixed bilayers containing 20 mol % POPG plus 80 mol % α-CD_2-POPC at various $CaCl_2$ concentrations (plus 100 mM NaCl and 10 mM Tris-HCl, pH 7.4, 298 K).

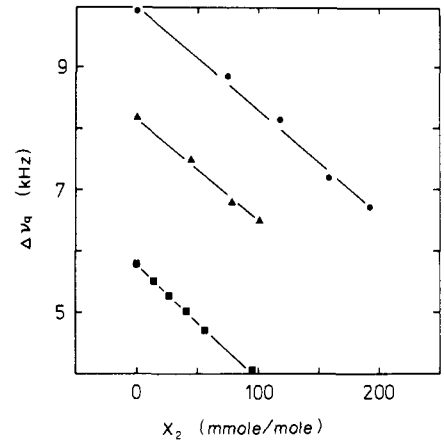

FIGURE 6: Deuterium quadrupole splittings, $\Delta\nu_Q$, of α-CD_2-POPC, in various mixtures with POPG at 298 K, as a function of the bound calcium, X_2. Squares, 100% POPC, $\Delta\nu_Q = 5.8 - 20.5X_2$; triangles, 80% POPC plus 20% POPG, $\Delta\nu_Q = 8.1 - 16.7X_2$; circles, 50% POPC plus 50% POPG, $\Delta\nu_Q = 9.9 - 17.3X_2$. Lipid proportions are in mole percent, $\Delta\nu_Q$ in kilohertz, and X_2 in moles of calcium per mole of lipid. The 100% POPC data were taken from Altenbach and Seelig (1984).

that the different polar lipid head groups interact, that they engage in a mutual perturbation, and that their conformation in a mixture of lipid species is not equivalent to that in a bilayer membrane consisting of a single species.

The series of ^2H NMR spectra shown in Figure 5 illustrates the effects of calcium on the quadrupole splitting in a mixture of 20 mol % POPG plus 80 mol % α-CD_2-POPC. In the absence of calcium, the quadrupole splitting amounts to 8.1 kHz. Upon addition of calcium, the quadrupole splitting decreases progressively with increasing calcium concentration and reverses its sign at higher calcium concentrations. Since only the absolute value of the quadrupole splitting is available from ^2H NMR, the assignment of a positive quadrupole splitting to α-CD_2-POPC in the absence of calcium is purely arbitrary.

The spectra shown in Figure 5 are each characteristic of lipids in a liquid-crystalline bilayer even at quite high calcium concentrations. In pure phosphatidylglycerol bilayers, the presence of low concentrations of calcium (i.e., 10 mM) induces a complex phase behavior and increases the temperature of the gel to liquid-crystal phase transition by more than 40 °C (Van Dijk et al., 1978; Fleming & Keough, 1983; Borle & Seelig, 1985). This stricture is relieved upon mixing phosphatidylglycerol with as little as 20 mol % phosphatidylcholine (Borle & Seelig, 1985). The phase transitions of both POPC and POPG remain well below room temperature in such mixtures, even upon the addition of high concentrations of calcium, as has been determined by using both differential scanning calorimetry and NMR techniques [see, for example, Figure 3 and Borle & Seelig (1985)]. Thus, it is possible to observe liquid-crystalline-type ^2H NMR spectra in these mixtures and to measure quadrupole splittings even at high calcium concentrations. Moreover, in the range of calcium concentrations studied, a decrease in signal intensity (indicative of head group immobilization due to the onset of the gel to liquid-crystalline phase transition) was *not* observed until the temperature was decreased to below 5 °C independent of whether the POPC or the POPG signal was monitored.

A single quadrupole splitting was observed for each phospholipid type at each calcium concentration. Thus, the rate of exchange of lipid between the "calcium-bound" and the "free" state must be fast on the ^2H NMR time scale of 10^{-5}–10^{-6} s. This observation implies that there does not exist some fraction of the lipid population which is completely physically sequestered from binding calcium. This does not preclude the existence of discrete populations with differing affinities for calcium; rather, it imposes the constraint that equilibration between such lipid populations be rapid on the ^2H NMR time scale.

In order to utilize the change in quadrupole splitting as a measure of calcium binding, it is necessary to calibrate it with respect to the number of bound calcium ions. Figure 6 shows plots of the quadrupole splitting, $\Delta\nu_Q$, of the α-segment of head group deuteriated POPC vs. X_2 (determined by using atomic absorption spectroscopy), both parameters measured on the same samples, for various mixtures of POPC plus POPG (this calibration was not performed in the case of 80 mol % POPG plus 20 mol % POPC). We have performed the calibration only with respect to those data obtained below a calcium concentration of 50 mM in which region the atomic absorption binding assay remains reliable. A linear function of the general form

$$\Delta\nu_Q = \Delta\nu_0 - mX_2 \qquad (13)$$

was found in each case to be adequate to describe the relationship between $\Delta\nu_Q$, the quadrupole splitting of α-CD_2-POPC, and X_2, the amount of bound calcium, where $\Delta\nu_0$ is the quadrupole splitting in the absence of calcium. The values of $\Delta\nu_0$ and m were determined by using linear regression analysis. The values of $\Delta\nu_0$ were found to agree with those expected from the results shown in Figure 4. The slopes (m) determined for the various mixtures were nearly identical within experimental error, corresponding to −20.5 kHz (−16.7 kHz, −17.3 kHz) for bilayers consisting of 100% POPC (80 mol % POPC plus 20 mol % POPG; 50 mol % POPC plus 50 mol % POPG). The linearity of this relationship holds for every POPG–POPC mixture over approximately the same range of $0 < X_2 < 100$ mmol/mol. At greater levels of calcium binding, nonlinearities appear which are related to the inaccuracies in the determination of X_2 using atomic absorption spectroscopy as discussed earlier. We have restricted our calibration to values of X_2 smaller than 100 mM/M. A linear relationship between the quadrupole splitting $\Delta\nu_Q$ and the amount of bound ion has been demonstrated previously for the binding to POPC bilayers of calcium in the range up to 100 mM (Altenbach & Seelig, 1984) and tetraphenylphosphonium in the range up to 50 mM (Altenbach & Seelig, 1985). Extrapolation of the linear relationship between $\Delta\nu_Q$ and X_2 to include concentrations at which X_2 cannot be independently measured is clearly an assumption and can only be justified on the basis of the consistent molecular picture

Table I: Binding of Ca^{2+} to Mixtures of 20 mol % POPG plus 80 mol % α-CD_2-POPC (0.1 M NaCl and 0.01 M Tris-HCl, pH 7.4, 25 °C)

$C_{2,eq}$[a] (M)	$\Delta\nu_Q$ (kHz)	X_2[b] (M/M)	ψ_0[c] (mV)	$C_{2,M}$[c] (M)
0	8.10	0	−54.6	0
0.0012	7.40	0.042	−10.0	0.0026
0.0040	6.80	0.078	−1.2	0.0044
0.0161	6.40	0.102	11.2	0.0067
0.0425	5.70	0.144	20.2	0.0098
0.094	5.20	0.174	27.0	0.0115
0.184	4.30	0.227	32.1	0.0151
0.255	3.90	0.251	34.3	0.0176
0.355	3.10	0.299	36.3	0.0210
0.525	2.50	0.335	38.4	0.0265
0.717	1.90	0.371	39.7	0.0325
0.892	1.00	0.425	40.6	0.0379
1.60	−0.75	0.530		
2.25	−2.70	0.635		

[a] Measured by using atomic absorption spectroscopy. [b] Calculated with $\Delta\nu_Q = 8.1 - 16.7X_2$. [c] Calculated by using the parameters listed in Table III.

Table II: Binding of Ca^{2+} to Mixtures of 50 mol % POPG plus 50 mol % α-CD_2-POPC (0.1 M NaCl and 0.01 M Tris-HCl, pH 7.4, 25 °C)

$C_{2,eq}$[a] (M)	$\Delta\nu_Q$ (kHz)	X_2[b] (M/M)	ψ_0[c] (mV)	$C_{2,M}$[c] (M)
0	9.90	0	−75.4	0
0.0005	8.90	0.058	−26.2	0.0038
0.0030	8.00	0.110	−11.4	0.0073
0.0125	7.20	0.156	2.8	0.0100
0.0455	6.60	0.191	16.0	0.0131
0.105	6.00	0.225	23.9	0.0164
0.211	5.10	0.277	29.7	0.0210
0.355	4.20	0.329	33.3	0.0265
0.452	3.70	0.358	34.8	0.0300
0.547	2.50	0.428		
0.572	2.j0	0.433		
0.752	1.40	0.491		
0.897	0.50	0.543		
1.627	−2.50	0.717		

[a] Measured by using atomic absorption spectroscopy. [b] Calculated with $\Delta\nu_Q = 9.9 - 17.3X_2$. [c] Calculated by using the parameters listed in Table III.

which emerges upon employment of equations similar to eq 13. A second implicit assumption of such an extrapolation is that the mode of calcium binding remains constant over the entire range of concentrations.

The numerical results of ^2H NMR measurements of the quadrupole splittings in mixtures of POPC plus POPG over a range of calcium concentrations are summarized in Tables I and II.

Discussion

The key experimental observations of this study are that increased calcium binding accompanies an increase in bilayer POPG content, that all bilayer lipids, not just POPG, experience the bound calcium, and that there is a rapid equilibrium between the bound and free states. Thus, calcium binding is a highly dynamic equilibrium where the ions must remain free or floating at the membrane surface. The central issues raised by these observations concern, first, whether calcium binding increases as a result of an intrinsically greater chemical affinity for POPG or as a result of electrostatics and, second, the precise mode of calcium binding.

Calcium Binding at Low Ca^{2+} Concentrations. In Figure 7, the Ca^{2+} binding isotherms for 20 and 50 mol % POPG (Tables I and II) and for pure POPC (Altenbach & Seelig, 1984) are plotted for the concentration range up to 100 mM Ca^{2+}. The solid lines represent computer simulations of the binding isotherms which were obtained by combining the

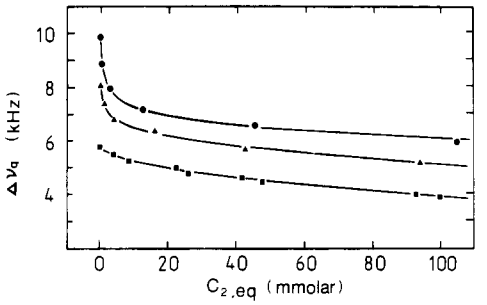

FIGURE 7: Calcium binding isotherms for various mixtures of POPC plus POPG and the corresponding computer simulations assuming a lipid/ion stoichiometry of 1. Squares, 100% POPC; triangles, 80% POPC plus 20% POPG; circles, 50% POPC plus 50% POPG. The average deviations of the data points from the simulation curves for $n = 1$ were 35 Hz at 100% POPC, 71 Hz at 80% POPC plus 20% POPG, and 76 Hz at 50% POPC plus 50% POPG. Other parameters were as listed in Table III.

Table III: Parameters of Best Fit to Calcium Binding Isotherms for Mixtures of POPG–POPC (0.1 M NaCl and 0.01 M Tris-HCl, pH 7.4, 25 °C)

mole fraction of POPC	1.0	0.8	0.5
mole fraction of POPG	0	0.2	0.5
effective fractional charge	0	0.20	0.34
m^* (kHz·C^{-1} m^2)[b]	43.5	35.5	36.7
$K_1 = K_{Na}$ (M^{-1})	0.15	0.85	0.62
$K_2 = K_{Ca}$ (M^{-1})	13.9 (12.4)[a]	19.5	18.8
lipid ion stoichiometry	2 (1)	1	1
χ (Hz)	68 (35)	109	46

[a] Numbers in parentheses refer to simulation of Ca^{2+} binding data for pure POPC bilayers using the nonspecific binding model eq 7 with $n = 1$ and restricting the simulation to $C_{Ca,eq} = 100$ mM. The full data set of POPC–Ca^{2+} binding was simulated with the specific binding model eq 9 with $n = m = 2$. The simulation with $n = 1$ is shown in Figure 7 and that with $n = m = 2$ in Figure 9. [b] Note: $m^* = mS/e^0$.

Gouy–Chapman theory, the Boltzmann equation, and the nonspecific binding model of eq 7 with $n = 1$. Sodium binding was also taken into account. The binding constants used for the simulation (actually obtained by the more comprehensive fit procedure outlined below) are summarized in Table III. For all three data sets in Figure 7, the simple Langmuir adsorption isotherm with a lipid to ion ratio of 1:1 and rather similar binding constants in the range of 12–20 M^{-1} yields a good agreement between theory and experiment. Clearly, the differences in the extent of Ca^{2+} binding which occur upon addition of POPG can be explained almost entirely in terms of electrostatic interactions as included in the Gouy–Chapman theory. It should be noted, however, that the 1:1 binding model is not unique. The limited concentration range represented in Figure 7 can be equally well simulated by using either a specific or a nonspecific binding model and values of the lipid to ion binding ratio equal to either 1, 2, or 3.

Determination of the Mode of Ca^{2+} Binding. The precise mode of ion binding can be determined provided that the binding isotherm can be measured up to high Ca^{2+} concentrations. The experimental data can then be compared with computer simulations of various binding models, and the quality of the computer fit can be judged from the average deviation (χ) between the theoretical prediction and the experimentally determined binding isotherm. Figure 8 illustrates the manner in which the effective mechanism of Ca^{2+} binding could be differentiated for the particular case of a bilayer composed of 80 mol % POPC plus 20 mol % POPG. Three different binding models were compared: two nonspecific models with lipid:Ca^{2+} ratios of 1:1 and 2:1 ($n = 1$ and $n = 2$, respectively, cf. eq 7) as well as a specific binding model with a 2:1 stoichiometry ($n = m = 2$, cf. eq 9). The interfacial

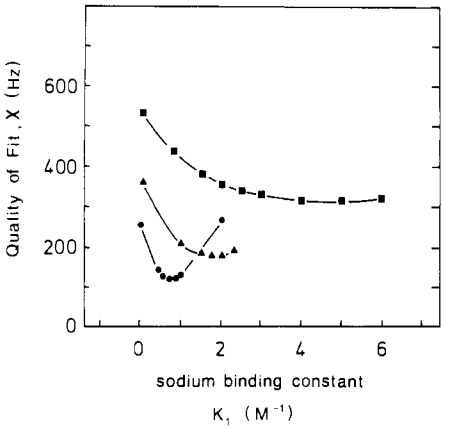

FIGURE 8: Average deviations of the data points, χ, for mixtures containing 80 mol % POPC plus 20 mol % POPG, as a function of the entered sodium association constant, K_1, in computer simulations of the calcium binding isotherm. Circles, $n = 1$; triangles, $n = 2$, unspecific binding; squares, $n = 2$, specific binding. The apparent mole fraction of negative lipid was held constant at 0.20, and the calibrated slope was as indicated in Table III.

concentration of metal ions was calculated by means of the Gouy–Chapman theory. The competitive binding of Na^+ was also taken into account. For a given model and a given sodium binding constant, the best computer fit to the experimental data was determined. As a result of this computer simulation, the Ca^{2+} binding constant as well as the average deviation χ was obtained. Figure 8 then displays the variation of χ with the sodium binding constant for the three models investigated. Two conclusions can be drawn from this comparison. First, the computer simulations allow a decision between the three binding models. The best fit by far for this particular membrane is obtained for a nonspecific model with a lipid:Ca^{2+} ratio of 1:1 which is equivalent to a simple Langmuir adsorption isotherm. Second, a definite optimal sodium binding constant of $K_1 = 0.85\ M^{-1}$ could be demonstrated as manifested in the minimum of the χ vs. K_1 curve.

Corresponding simulations were also performed for pure POPC bilayers and for an equimolar mixture of POPC and POPG. The best fits to the different Ca^{2+} binding isotherms for the whole concentration range investigated are shown in Figure 9. The corresponding parameters of fit are indicated in Table III. In the case of 50 mol % POPG, the data points above 0.5 M $CaCl_2$ were not included in the fit procedure. At this Ca^{2+} concentration, a marked discontinuity in the otherwise smooth Ca^{2+} binding isotherm was apparent with this mixture. As we remain uncertain about the origin of this effect, we have refrained from attempting an analysis of these data.

The lipid/Ca^{2+} stoichiometries listed in Table III imply a fundamental difference in the mode of Ca^{2+} binding between pure POPC vs. mixed POPC–POPG bilayers. Ca^{2+} binding to POPC bilayers over the whole concentration range can be best described in terms of formation of a ternary complex involving complexation of two lipids to one calcium ion (Altenbach & Seelig, 1984). The addition of a sodium competition term has not changed this conclusion. However, if Ca^{2+} concentrations up to 100 mM are considered, the data can be equally well explained by a 1:1 binding mechanism (cf. Figure 7). In contrast, the Ca^{2+} binding to POPC–POPG mixtures can be best described by assuming a 1:1 stoichiometry regardless of the range of Ca^{2+} concentrations.

It can further be concluded (cf. Figure 8) that a distinct improvement in the computer simulation of Ca^{2+} binding isotherms is achieved by taking into account the competitive

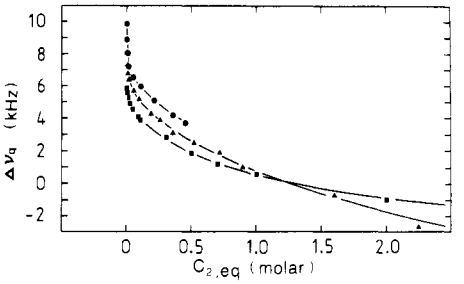

FIGURE 9: Calcium binding isotherms and best-fit computer simulations for various mixtures of POPC plus POPG. The simulation parameters were precisely those listed in Table III. Squares, 100% POPC; triangles, 80% POPC plus 20% POPG; circles, 50% POPC plus 50% POPG.

binding of Na^+. The optimal binding constants for Na^+ binding to pure POPC and mixed POPC–POPG bilayers are summarized in Table III. The Na^+ binding constants are 1–2 orders of magnitude smaller than the corresponding Ca^{2+} binding constants.

Finally, it may be noted from Table III that for equimolar POPC–POPG membranes the effective negative charge for an optimal computer fit was 30% smaller than expected on the basis of the POPG content. Furthermore, analysis of the atomic absorption spectroscopy calcium binding data for bilayers containing 80 mol % POPG plus 20 mol % POPC showed a 30–35% disparity between the expected and apparent values of X_{PG}. These findings tend to indicate that, at high negative surface charge densities, the acidic phospholipids remain incompletely dissociated. However, this effect may be more apparent than real and, when observed previously (Cowley et al., 1978; Parsegian, 1973), was rationalized by assuming a model which permitted the counterions to percolate *behind* the lipid phosphate groups, effectively reducing the apparent surface density without having to invoke incomplete dissociation of the acidic phospholipids.

Comparison with Earlier Studies. The binding of Ca^{2+} to membranes composed of PG (with the fatty acid composition of egg lecithin) has been studied by measuring its effect on the electrophoretic mobility of sonicated vesicles (Lau et al., 1981). The Ca^{2+} binding constant could be estimated, in a simple and straightforward fashion, as corresponding to the reciprocal of the calcium concentration at which the ζ potential of the negatively charged vesicles reversed its sign, assuming a 1:1 complex. This charge reversal occurred in the range of 0.1–0.2 M. A more detailed analysis using the Gouy–Chapman theory yielded intrinsic association constants for Ca^{2+} and Na^{2+} of $K_{Ca} = 8.5\ M^{-1}$ and $K_{Na} = 0.6\ M^{-1}$, respectively, based on a data set of up to 100 mM Ca^{2+}. This compares favourably with the present results of $K_{Ca} = 19.5\ M^{-1}$ ($18.5\ M^{-1}$) and $K_{Na} = 0.85\ M^{-1}$ ($0.62\ M^{-1}$) for a POPG–POPC membrane with 20 mol % (50 mol %) POPG in 0.1 M NaCl + 0.01 M Tris buffer.

Our investigations differ from these earlier studies in the following respects: (1) Lipids having a homogeneous fatty acid composition, with a saturated *sn*-1 palmitoyl and an unsaturated *sn*-2 oleoyl chain, were employed. (2) Mixtures of POPC and POPG rather than pure PG membranes were studied. In particular, those POPC–POPG mixtures containing 20% POPG mimic the approximate charge composition of biological membranes. (3) The calcium binding isotherms could be measured directly and up to high concentrations. This allowed a quantitative comparison between various binding models. Measurements up to 0.1 M Ca^{2+} are not sufficient to differentiate unambiguously the different possible binding models. (4) For membranes with POPG contents >50%, the present

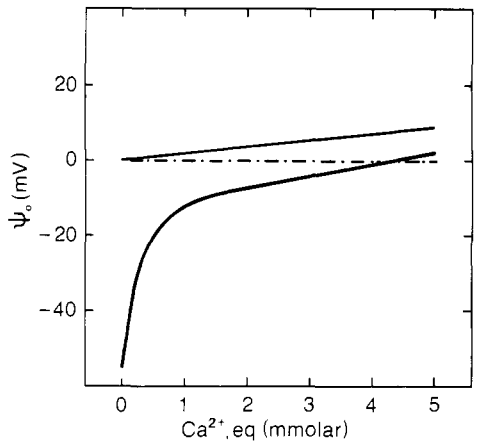

FIGURE 10: Surface potential, ψ_0, for mixtures of 80 mol % POPC plus 20 mol % POPG (lower curve) and for 100% POPC (upper line) as a function of the equilibrium bulk calcium concentration. Surface potentials were calculated by using the parameters of Table III. The dashed line is the zero reference.

studies indicate that the effective membrane surface charge is smaller than expected on the basis of the POPG content. This could be the effect of only partial dissociation of POPG in the multilayer dispersions or of a percolation of positively charged metal ions behind the phosphate groups. Such an effect was not noted in the electrophoretic mobility studies.

Depiction of the Membrane Surface. The ^2H NMR spectra reveal the state of the membrane lipids upon Ca^{2+} binding. Under all conditions, a liquid-crystalline bilayer conformation is indicated for both POPC and POPG. Ca^{2+} induces a conformational change of both the choline and glycerol head groups. The collapse of the quadrupole splitting of α-CD_2-POPC at about 2 M Ca^{2+} (cf. Figure 5) and its reappearance at even higher concentrations demonstrate that the C–D bond vectors are inclined at close to the magic angle with respect to the bilayer normal. At this orientation, changes of the torsion angles by 5–15° can easily account for the experimentally observed variations of the quadrupole splittings of α-CD_2-POPC and β-CD-POPG [cf. Akutsu & Seelig (1981)].

^2H NMR studies further provide insight into the mechanism and dynamics of Ca^{2+} binding. On the time scale of the NMR experiments, the Ca^{2+} ions remain mobile, floating in a trough of the electrical potential at the membrane surface. The association of Ca^{2+} with mixed POPC–POPG membranes leads to a uniform change of the membrane surface. Local effects such as preferential binding of Ca^{2+} to POPG molecules can be excluded.

Biological Implications. Finally, the reciprocal interdependence of Ca^{2+} binding and the surface potential deserve consideration. Figure 10 illustrates the variation of ψ_0 with the equilibrium bulk Ca^{2+} concentration for the biologically relevant case of Ca^{2+} binding to a POPC (80 mol %)–POPG (20 mol %) mixture as well as for binding to a pure POPC membrane. In the absence of Ca^{2+}, the surface potential is initially about −55 mV for the POPC–POPG mixture. The addition of as little as 1 mM Ca^{2+} increases this value by 40 mV, and at 10 mM Ca^{2+}, the surface potential has not just been neutralized but actually assumes a positive value. For 100% POPC bilayers, the surface is originally neutral, and the surface potential increases slowly, almost linearly as the calcium concentration is increased. The sharply contrasting behavior in these two situations accentuates the sensitivity of the surface potential of membranes containing negative lipids to the binding of calcium. The importance of the surface potential in the modulation of the voltage-dependent conductance of various Na^+, K^+, and Ca^{2+} channels has been discussed by Hille (1984). For example, addition of 2 mM Ca^{2+} causes a shift of +15 mV in the voltage dependence of the conductance of Na^+ channels isolated from frog skeletal muscle. Thus, altering the surface potential via Ca^{2+} binding may represent a means of effecting membrane-dependent biological processes.

Conversely, altering the surface potential influences the extent of Ca^{2+} binding. Compare the Ca^{2+} binding to the above 20% POPG mixture with that which occurs to pure POPC membranes at the two Ca^{2+} concentrations, 2 and 10 mM. (These concentrations encompass the range of typical Ca^{2+} concentrations outside the cell.) For pure POPC bilayers, the amount of Ca^{2+} bound to the membrane surface would be 8 and 28 mmol of Ca^{2+}/mol of POPC, respectively, for the two concentrations [0.1 M NaCl, 25 °C; cf. Altenbach & Seelig (1984)]. In contrast, a much higher Ca^{2+} loading of the membrane surface is observed for the POPC–POPG mixture with 50 and 80 mmol of Ca^{2+} bound per mole of total lipid. The "excess" surface Ca^{2+} is greatest at very low Ca^{2+} concentrations. Thus, negative lipids such as PG may play a biological role as enhancers of the Ca^{2+} concentrations at the membrane surface.

ACKNOWLEDGMENTS

We thank P. Ganz and R. Jenni for their expert technical assistance and E. Aebischer for patiently preparing the manuscript. We are grateful to Dr. J. Pavel, Ciba-Geigy AG, Basel, for performing the atomic absorption spectroscopy measurements.

Registry No. POPC, 26853-31-6; POPG, 81490-05-3; Na, 7440-23-5; Ca, 7440-70-2.

REFERENCES

Altenbach, C., & Seelig, J. (1984) *Biochemistry 23*, 3913–3920.

Altenbach, C., & Seelig, J. (1985) *Biochim. Biophys. Acta 818*, 410–415.

Aveyard, R., & Haydon, D. A. (1973) *An Introduction to the Principles of Surface Chemistry*, Cambridge University Press, Cambridge, England.

Bevington, P. R. (1969) *Data Reduction and Error Analysis for the Physical Sciences*, McGraw-Hill, New York.

Borle, F., & Seelig, J. (1985) *Chem. Phys. Lipids 36*, 263–283.

Comfurius, P., & Zwaal, R. F. A. (1977) *Biochim. Biophys. Acta 488*, 36–42.

Cowley, A. C., Fuller, N. L., Rand, R. P., & Parsegian, V. A. (1978) *Biochemistry 17*, 3163–3168.

Davis, J. H., Jeffrey, K. R., Bloom, M., Valic, M. I., & Higgs, T. P. (1976) *Chem. Phys. Lett. 42*, 390–394.

Eisenberg, M., Gresalfi, T., Riccio, T., & McLaughlin, S. (1979) *Biochemistry 18*, 5213–5223.

Fleming, B. D., & Keough, K. M. (1983) *Can. J. Biochem. 61*, 882–891.

Grasdalen, H., Eriksson, L. E. G., Westman, J., & Ehrenberg, A. (1977) *Biochim. Biophys. Acta 469*, 151–162.

Hille, B. (1984) *Ionic Channels of Excitable Membranes*, Chapter 13, Synauer Assoc., Sunderland, MA.

Hitchcock, C., & Nichols, B. W. (1971) in *Plant Lipid Biochemistry*, Chapter 3, Academic Press, London.

Lau, A., McLaughlin, A., & McLaughlin, S. (1981) *Biochim. Biophys. Acta 645*, 279–292.

Lennarz, W. J. (1970) in *Lipid Metabolism* (Wakil, S. I., Ed.) Chapter 5, Academic Press, London.

Lis, L. J., Parsegian, V. A., & Rand, R. P. (1981a) *Biochemistry 20*, 1761–1770.

Lis, L. J., Lis, W. T., Parsegian, V. A., & Rand, R. P. (1981b) *Biochemistry 20*, 1771–1777.
Lowenstein, W. R. (1984) *Curr. Top. Membr. Transp. 21*, 221–252.
McElhaney, R. N. (1982) *Chem. Phys. Lipids 30*, 229–287.
McLaughlin, A., Eng, W. K., Vaio, G., Wilson, T., & McLaughlin, S. (1983) *J. Membr. Biol. 76*, 183–193.
McLaughlin, S. A. (1977) *Curr. Top. Membr. Transp. 9*, 71–144.
McMurray, W. C. (1973) in *Form and Function of Phospholipids* (Ansell, G. B., Hawthorne, J. N., & Dawson, R. M. C., Eds.) Chapter 4, Elsevier, Amsterdam, The Netherlands.
Oshima, H., & Mitsui, T. (1978) *J. Colloid Interface Sci. 63*, 525–537.
Overbeek, J. T. G. (1952) in *Colloid Science* (Kruyt, H. R., Ed.) Vol. 1, Chapter 5, Elsevier, Amsterdam, The Netherlands.
Parsegian, V. A. (1973) *Annu. Rev. Biophys. Bioeng. 2*, 222–255.
Rand, R. P. (1981) *Annu. Rev. Biophys. Bioeng. 10*, 277–314.
Rouser, G., Nelson, G. J., Fleischer, S., & Simon, G. (1968) in *Biological Membranes* (Chapman, D., Ed.) Chapter 1, Academic Press, London.
Scarpa, A., & Carafoli, E. (1978) *Ann. N.Y. Acad. Sci. 307*, 1–655.
Seelig, J. (1977) *Q. Rev. Biophys. 10*, 353–418.
Seelig, J., Tamm, L., Hymel, L., & Fleischer, S. (1981) *Biochemistry 20*, 3922–3933.
Silvius, J. R. (1982) in *Lipid–Protein Interactions* (Jost, P. C., & Griffith, O. H., Eds.) Vol. 2, Chapter 5, Wiley, New York.
Sixl, F., & Watts, A. (1983) *Proc. Natl. Acad. Sci. U.S.A. 80*, 1613–1615.
Somylo, A. P. (1985) *Nature (London) 309*, 516–517.
Stankowski, S. (1983a) *Biochim. Biophys. Acta 735*, 341–351.
Stankowski, S. (1983b) *Biochim. Biophys. Acta 735*, 352–361.
Stankowksi, S. (1984) *Biochim. Biophys. Acta 777*, 167–182.
Strickland, K. (1973) in *Form and Function of Phospholipids* (Ansell, G. B., Hawthorne, J. N., & Dawson, R. M. C., Eds.) Chapter 2, Elsevier, Amsterdam, The Netherlands.
Tamm, L. K., & Seelig, J. (1983) *Biochemistry 22*, 1474–1483.
Van Dijck, P. W. M., de Kruijff, B., Verkleij, A. J., Van Deenen, L. L. M., & de Gier, J. (1978) *Biochim. Biophys. Acta 512*, 84–96.
Wohlgemuth, R., Waespe-Sarcevic, N., & Seelig, J. (1980) *Biochemistry 19*, 3315–3321.

Mechanism of Transfer of Reduced Nicotinamide Adenine Dinucleotide among Dehydrogenases. Transfer Rates and Equilibria with Enzyme–Enzyme Complexes†

D. K. Srivastava and S. A. Bernhard*
Institute of Molecular Biology, University of Oregon, Eugene, Oregon 97403
Received May 29, 1986; Revised Manuscript Received November 10, 1986

ABSTRACT: The direct transfer of NADH between A–B pairs of dehydrogenases and also the dissociation of NADH from individual E–NADH complexes have been investigated by transient stopped-flow kinetic techniques. Such A–B transfers of NADH occur without the intermediate dissociation of coenzyme into the aqueous solvent environment [Srivastava, D. K., & Bernhard, S. A. (1985) *Biochemistry 24*, 623–628]. The equilibrium distributions of limiting NADH among aqueous solvent and A and B dehydrogenase sites have also been determined. At sufficiently high but realizable concentrations of dehydrogenases, both the transfer rate and the equilibrium distribution of bound NADH are virtually independent of the excessive enzyme concentrations; at excessive E_2 concentration, substantial NADH is bound to the E_1 site. These results further substantiate earlier kinetic arguments for the preferential formation of an E_A–NADH–E_B complex, within which coenzyme is directly transferred between sites. The unimolecular specific rates of coenzyme transfer from site to site are nearly invariant among different A–B dehydrogenase pairs. The equilibrium constants for the distribution of coenzyme within the E_A·E_B complexes are near unity. At high $[E_2]$ and for $[E_2] > [E_1] > [NADH]$, E_1–NADH·E_2 and E_1·NADH–E_2 are virtually the only coenzyme-contained species. In contrast to the nearly invariant unimolecular NADH transfer rates within E_A·E_B complexes, unimolecular specific rates of dissociation of NADH from E–NADH into aqueous solution are highly variable. The specific rate of coenzyme transfer within the E_A·E_B complex can be either substantially greater than or substantially less than the rate of coenzyme dissociation from E_1–NADH into the aqueous environment. Thus, enzyme–enzyme interactions within the A–B pairs modulate the rate of coenzyme transfer.

In previous communications from this laboratory, we have shown that the utilization of NADH, in the form of the E_1–NADH complex, can proceed at velocities very much greater than that predicted from the known dissociation constant of E_1–NADH and the Michaelian parameters for the E_2-catalyzed hydrogenation of S_2 by the available aqueous NADH (Srivastava & Bernhard, 1984, 1985) (eq 1). This

$$E_1\text{-NADH} + S_2 \xrightarrow{E_2} E_1\text{-NAD}^+ + P_2 \qquad (1)$$

enhanced velocity via direct transfer is operative whenever the

† This work was supported by grants from the U.S. Public Health Service of the National Institutes of Health (GM37056) and from the National Science Foundation (PCM801-6249). A preliminary account of this work has been presented at the NATO Symposium on "The Organization of Cellular Metabolism" in 1985.

0006-2960/87/0426-1240$01.50/0